Neuron
Article

Motor Cortex Gates Vibrissal Responses in a Thalamocortical Projection Pathway

Nadia Urbain[1] and Martin Deschênes[1,*]
[1]Centre de Recherche Université Laval Robert-Giffard, Québec City, Canada G1J 2G3
*Correspondence: martin.deschenes@crulrg.ulaval.ca
DOI 10.1016/j.neuron.2007.10.023

SUMMARY

Higher-order thalamic nuclei receive input from both the cerebral cortex and prethalamic sensory pathways. However, at rest these nuclei appear silent due to inhibitory input from extrathalamic regions, and it has therefore remained unclear how sensory gating of these nuclei takes place. In the rodent, the ventral division of the zona incerta (ZIv) serves as a relay station within the paralemniscal thalamocortical projection pathway for whisker-driven motor activity. Most, perhaps all, ZIv neurons are GABAergic, and recent studies have shown that these cells participate in a feedforward inhibitory circuit that blocks sensory transmission in the thalamus. The present study provides evidence that the stimulation of the vibrissa motor cortex suppresses vibrissal responses in ZIv via an intra-incertal GABAergic circuit. These results provide support for the proposal that sensory transmission operates via a top-down disinhibitory mechanism that is contingent on motor activity.

INTRODUCTION

It is often said that the thalamus is the gateway to the cerebral cortex. This holds as a rule for the first-order thalamic nuclei, which receive sensory input and convey information to specific cortical areas. In regards to the higher-order thalamic nuclei, however, the case is more ambiguous, because most of these nuclei receive driver input from both the cerebral cortex and prethalamic sensory stations (Guillery, 2005). Moreover, sensory transmission in these nuclei seems to be normally disabled, at least in the anesthetized animal, by inhibitory inputs of extrathalamic origin. This is the case, for instance, for the posterior nuclear group (Po) in rodents, in which the relay of vibrissal messages is impeded by inhibitory inputs that arise from a subthalamic region called the zona incerta (ZI; Trageser and Keller, 2004; Lavallée et al., 2005). The control of this inhibitory process, known as sensory gating, is the focus of the present study.

The ventral division of ZI (ZIv) receives vibrissal input from the interpolaris subnucleus of the brainstem trigeminal complex (SpVi), and projects to Po (Kolmac et al., 1998; Power et al., 1999; Veinante et al., 2000a; Barthó et al., 2002; Lavallée et al., 2005). Most, perhaps all, ZIv cells are GABAergic (Nicolelis et al., 1995; Kolmac and Mitrofanis, 1999), and recent studies have shown that incertal cells take part in a feedforward inhibitory circuit that blocks sensory transmission through Po (Trageser and Keller, 2004; Lavallée et al., 2005). It was thus proposed that the relay of vibrissal inputs in this higher-order thalamic nucleus relies on a mechanism of disinhibition (i.e., inhibition of the inhibitory incerto-thalamic pathway). This proposal raises two issues: the first concerns the anatomical substrate of disinhibition, and the second relates to the behavioral context under which disinhibition occurs.

A state-dependent gating hypothesis was proposed, which states that inhibition of ZIv cells is mediated by brainstem cholinergic neurons that increase their firing rate on arousal (Trageser et al., 2006). Accordingly, sensory transmission in Po would be reinstated when animals are awake. In support of this hypothesis, stimulation of the brainstem cholinergic groups or iontophoretic application of carbachol in anesthetized animals were both found to depress incertal cells' excitability and to enhance sensory transmission in Po (Trageser et al., 2006; Masri et al., 2006).

An alternative hypothesis was also proposed, which rests on the premise that Po relays vibrissal inputs that are contingent on motor activity (active touch). Accordingly, corticofugal messages that modulate vibrissa motion during palpation would activate inhibitory cells that contact ZIv neurons, thus creating a window of disinhibition in Po (Lavallée et al., 2005). Although GABAergic synapses have been observed on ZIv somata (Lavallée et al., 2005), their origin remains as yet undetermined, and there still exists no evidence that corticofugal discharges from any cortical area can suppress whisker-evoked activity in ZIv. The present study provides such evidence by showing that stimulation of the vibrissa motor cortex suppresses vibrissal responses in ZIv, and that suppression is mediated by an intra-incertal GABAergic circuit.

RESULTS

The first part of the results considers vibrissal response properties in ZIv. The second part examines how these responses are affected by motor cortex stimulation.

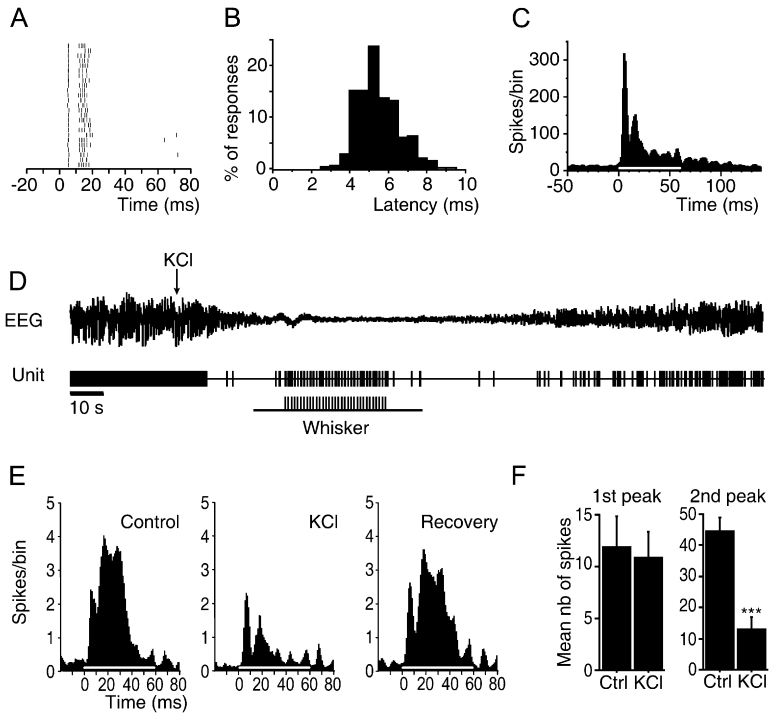

Figure 1. Properties of Vibrissal Responses in ZIv

(A) Peristimulus time raster of 25 responses evoked in a ZIv cell by deflecting vibrissa D3. (B) Distribution of the onset latency of all vibrissal responses (237 vibrissae, 44 cells). Population peristimulus time histogram (PSTH) in (C) shows the bimodal profile of the responses evoked in 44 cells by deflection of the dominant vibrissa in the best direction (white bar). (D) The effect of cortical spreading depression on the activity of a ZIv cell. Note that the cell kept responding to whisker deflection during cortical inactivation. Population PSTHs in (E) depict the effect of cortical-spreading depression on the vibrissal responses of 17 ZIv cells that displayed a prominent secondary peak in their responses. The first peak in the PSTHs was not significantly depressed by cortical inactivation, while the second peak was ($p < 0.001$; bar graphs in [F]). The mean number of spikes evoked in 17 cells within time windows of 0–10 ms (first peak) and 10–25 ms (second peak) was used to build the graphs. Error bars in (F) = SEM.

Size and Topography of Vibrissal Receptive Fields

In deeply anesthetized rats, whisker-responsive ZIv cells displayed a low level of spontaneous activity (mean firing rate estimated over a 3 min period in 25 cells: 10.0 ± 2.6 spikes/s), which consisted of periodic spike trains that were time related to the high-voltage rhythmic electroencephalographic (EEG) waves (0.5–3 Hz) recorded in the barrel cortex (see also Barthó et al., 2007). Manual deflection of individual vibrissae revealed that all whisker-sensitive cells responded to multiple whiskers (mean receptive field size: 10.35 ± 1.0 vibrissae, range 3–19; 57 cells tested). Receptive fields were asymmetric; they commonly included five to six vibrissae within a row, but rarely more than three vibrissae within an arc. To assess this feature quantitatively, we computed a receptive field symmetry index, estimated as the number of vibrissae within the longest row divided by that in the longest arc. A symmetry index of 1.97 ± 0.11 was obtained, confirming that the receptive field of ZIv cells contains, on average, twice as many vibrissae within a row than within an arc.

Latency and Magnitude of Sensory Responses; Role of Cortex

Controlled deflection of the vibrissae induced robust responses in ZIv cells, consisting of one to three short-latency action potentials (Figure 1A; mean onset latency for 237 whiskers at all directions: 5.46 ± 0.05 ms [Figure 1B]; mean onset latency for the shortest latency responses evoked by the dominant whiskers: 4.20 ± 0.11 ms) that were often followed 6–15 ms later by a single spike or a burst of two to five action potentials (raster display in Figure 1A). The population peristimulus time histogram (PSTH; Figure 1C) shows the bimodal profile of the responses evoked in 44 cells by deflection of the dominant vibrissae in the best direction. Because corticofugal cells were previously shown to exert a strong drive in ZIv (Barthó et al., 2007), we examined the possibility that the second peak of excitation might arise from cortical feedback. This issue was addressed by silencing cortical cells while recording 17 ZIv cells that displayed a prominent secondary peak in their response to whisker deflection. Within 10 to 30 s after topical application of KCl on the barrel cortex, the EEG flattened and spontaneous discharges of ZIv neurons markedly diminished, but cells maintained robust short-latency responses to whisker stimulation (Figure 1D). Cortical inactivation, however, totally suppressed the second peak of excitation in nine cells, and clearly depressed its amplitude in the remaining eight cells. The second peak progressively reappeared as cortical slow-wave activity recovered (Figures 1E and 1F). Thus, this result indicates that the short-latency peak of excitation reflects direct activation by ascending trigeminal afferents, while the second peak is mediated, at least in part, by cortical feedback.

To exclude the potential contribution of cortical feedback to sensory responses, a poststimulus time window of 10 ms was used to compare the magnitude of the responses produced by the deflection of individual vibrissae. Controlled deflection of each vibrissa that composed the receptive field of a cell always revealed a gradient of response magnitude, with one of the vibrissae eliciting the largest response. PSTHs in Figure 2A show the total number of spikes (sum of all directions) evoked in a ZIv cell by each of the four vibrissae tested in the D row. Since

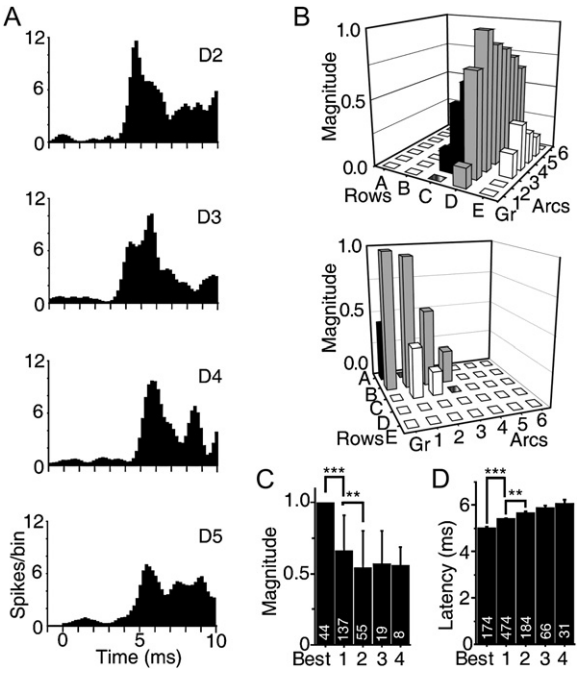

Figure 2. Gradient of Response Magnitude within the Receptive Field of ZIv Cells

PSTHs in (A) show the total number of spikes (sum of all directions) evoked in a ZIv cell by the deflection of four vibrissae tested in the D row. (B) 3D bar graphs of normalized response magnitudes within the receptive field of two incertal cells. For each vibrissa, response magnitudes were summed across all directions. Bars with zero magnitude indicate vibrissae with a threshold too high to be tested with the piezo stimulator. The histogram in (C) shows how response magnitude, as measured in (B), diminishes as distance from the dominant vibrissa increases (dominant vibrissa, best in [C] and [D]). The histogram in (D) shows how response latency increases as distance from the dominant vibrissa increases. Error bars in (C) and (D) indicate 1 SEM (***$p < 0.001$; **$p < 0.01$). The number of vibrissae is indicated within each bar.

deflection involved vibrissae of increasing remoteness from the dominant vibrissa (D2), response magnitude decreased and onset latency increased. The 3D bar graphs (Figure 2B) provide representative ensemble views of the distribution of normalized response magnitudes across the receptive field of two ZIv units. For the whole population of neurons (n = 44 cells), a significant difference in response magnitude was found between the dominant vibrissa and immediately adjacent vibrissae (ANOVA; $p < 0.001$; Figure 2C; note: in the center of the pad each vibrissa is surrounded by eight adjacent vibrissae). Furthermore, a significant difference was also found between the adjacent vibrissae and those situated one step away on the mystacial pad (ANOVA; $p < 0.01$). For the same population of cells (n = 44), response latencies displayed a similar gradient for the nondominant vibrissae. The histogram of Figure 2D shows how onset latencies (all vibrissae in all directions) increased as one moves away from the dominant whisker. Here again, the difference in onset latency was statistically significant between the responses elicited by the dominant vibrissa and immediately adjacent vibrissae (ANOVA; $p < 0.001$), and between the latter and those situated one step away on the mystacial pad (ANOVA; $p < 0.01$).

Angular Tuning of Vibrissal Responses

It was previously reported that SpVi cells possess a high degree of sensitivity to the direction of vibrissa deflection (Furuta et al., 2006). We thus explored the extent to which ZIv responses reflect the directional tuning of trigeminal inputs. Figure 3A shows normalized polar plots and a vector graph comparing the directional tuning of the responses elicited by seven of the vibrissae that composed the receptive field of a representative cell. For each vibrissa, a direction selectivity index, D, was calculated as a measure of the directional tuning (Taylor and Vaney, 2002). D was defined as: $D = | \sum v_i / \sum r_i |$, where v_i are vector magnitudes pointing in the direction of the stimulus and having length r_i equal to the number of spikes recorded during that stimulus. D can range from 0, when the responses are equal in all stimulus directions, to 1, when a response is obtained only for a single stimulus direction. Thus, values for D approaching 1 indicate asymmetric responses over a small range of angles, and therefore sharper directional tuning. The mean value of D computed for 44 ZIv cells (n = 263 vibrissae) was 0.18 ± 0.01 (range: 0.002–0.812), indicating lower direction selectivity than that reported for interpolaris neurons (a mean D value of 0.49 ± 0.29 was computed for projection cells in the rostral sector of the SpVi; Furuta et al., 2006). However, if one considers only those responses with significant tuning (circular statistics; n = 73 vibrissae), the mean D value rose to 0.38 ± 0.02 ($p < 0.05$; Rayleigh's Uniformity Test).

The multivibrissa structure of receptive fields in the ZIv raises the issue of the consistency of angular tuning preference; that is, whether the direction of motion that elicits the largest response is the same for all the vibrissae in the receptive field of each cell. To address this question, we first built polar plots that were normalized with respect to the largest response evoked by the most effective vibrissa, and computed the vector sum of individual polar graphs. Next, by computing the vector sum of all vibrissa-associated vectors within the receptive field of a cell, a grand vector was obtained that represented the ensemble direction tuning of that cell. The consistency of direction preference was estimated by computing the absolute value of the difference in angle between each of the vibrissa-associated vectors and the grand vector. Among a sample of 44 ZIv cells analyzed in this way, median values of angular difference were 38°, with 61% of the vibrissae included in the range of 0°–50°.

We next examined whether ZIv cells exhibit an angular tuning bias for upward whisker motion, as has been shown for their interpolaris partners (Furuta et al., 2006). The polar distribution of all grand vectors indeed indicates an upward preference (Figure 3B), but the mean normalized responses in all directions show that this preference was not as strong as that manifested by interpolaris neurons

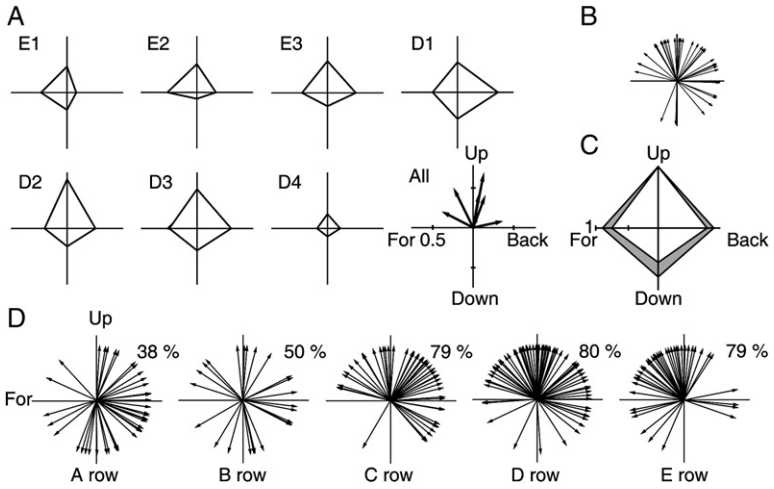

Figure 3. Angular Tuning of Vibrissal Responses in ZIv

Polar plots in (A) show normalized response magnitudes evoked by seven of the vibrissae that composed the receptive field of a ZIv cell (direction selectivity index of that cell: D = 0.2). The vector sum of each plot is depicted in the bottom right-hand polar graph (back, backward; down, downward; for, forward; up, upward). (B) Distribution of grand vectors of angular preference for 44 ZIv cells. The gray polar plot in (C) shows mean normalized responses in all directions of 44 ZIv cells (n = 263 vibrissae), whereas the white polar plot shows mean normalized responses for those vibrissae with a statistically significant tuning (n = 73 vibrissae). (D) Angular tuning of the responses evoked by vibrissae pertaining to different rows. Percentages above each plot indicate the proportion of vectors in the top quadrants. For vibrissae in rows C–E, but not forthose in rows A and B, vector response distributions significantly differ from a 50–50 division between the top and bottom quadrants (Chi test, $p < 0.001$ for rows C–D, and $0.1 < p < 0.2$ for rows A and B).

(gray polar plot in Figure 3C). However, if one considers only those responses with a statistically significant tuning (n = 73 vibrissae), the mean normalized responses in all directions display a clear upward preference (white polar plot in Figure 3C). When vector responses were sorted by row (Figure 3D), the response of ZIv cells exhibited a significant preference for the upward quadrants for the vibrissae in rows C–E (Chi test, $p < 0.001$), but not for those in rows A and B (Chi test, $0.1 < p < 0.2$). This upward preference was found in all rats.

In sum, whisker-sensitive ZIv cells possess row-oriented receptive fields, and exhibit responses which, albeit similar in several respects to those of SpVi neurons, differ from their presynaptic counterparts in being less direction selective and demonstrating a lower degree of angular preference for upward whisker motion. This suggests that synaptic mechanisms or input convergence transforms the afferent signal in ZIv.

Origin of Vibrissal Responses in ZIv: Effect of PrV and SpVi Lesions

Previous tract-tracing studies have shown that ZI receives trigeminal input not only from the SpVi, but also from the principalis nucleus (PrV; Roger and Cadusseau, 1985; Nicolelis et al., 1992; Williams et al., 1994; Veinante and Deschênes, 1999). We thus examined to what degree receptive field properties in ZIv were altered after elimination of each of these inputs. Parasagittal brainstem lesions were made medial to the PrV in three rats, so that the nucleus remained intact while ascending crossing axons were destroyed (Figure S1A in the Supplemental Data available with this article online). As estimated from cytochrome oxidase (CO)-stained horizontal sections of the brainstem, lesions extended rostrocaudally between the frontal planes 8 to 10.5 mm behind the bregma and throughout the depth of the brainstem. Recordings in the somatosensory thalamus further attested to the effectiveness of the lesion. In lesioned rats, none of the units recorded in Po or in the dorsal part of the ventral posterior medial nucleus (VPM) responded to whisker deflection, but cells with multiwhisker receptive fields were still present in the ventral lateral part of the VPM (VPMvl), which receives input from the caudal division of the SpVi (Veinante et al., 2000a). Analysis of the responses of 21 whisker-sensitive ZIv cells in PrV lesioned rats did not reveal any significant change in receptive field size and topography, or in onset latency and magnitude of the responses as compared with normal rats (see table in Figure S1). In contrast, a lesion of the trigeminal tract that prevented the activation of SpVi cells left ZIv cells totally unresponsive to whisker stimulation (53 incertal cells tested in three rats). Yet, some cells kept responding to stimulation of the nose and perioral region. Trigeminal tract lesions were made at the level of the oralis subnucleus, so as to severe the descending branches of primary afferent fibers, but keep intact vibrissal inputs to the PrV (Figure S1B). The effectiveness of the lesion was confirmed by recording cells with normal vibrissal receptive field in the dorsal VPM, and noting an absence of multiwhisker units in the VPMvl. In sum, lesion experiments indicate that vibrissal responses in ZIv critically depend on the integrity of the ascending pathway that arises from the SpVi.

To further assess this result, FluoroGold was injected into the ZI to map the precise location of retrogradely labeled cells in the PrV and SpVi. The three cases analyzed, in which the injection sites were confined to the ZI (Figure 4A), yielded similar results; retrogradely labeled cells in the SpVi were located in the rostral half of the

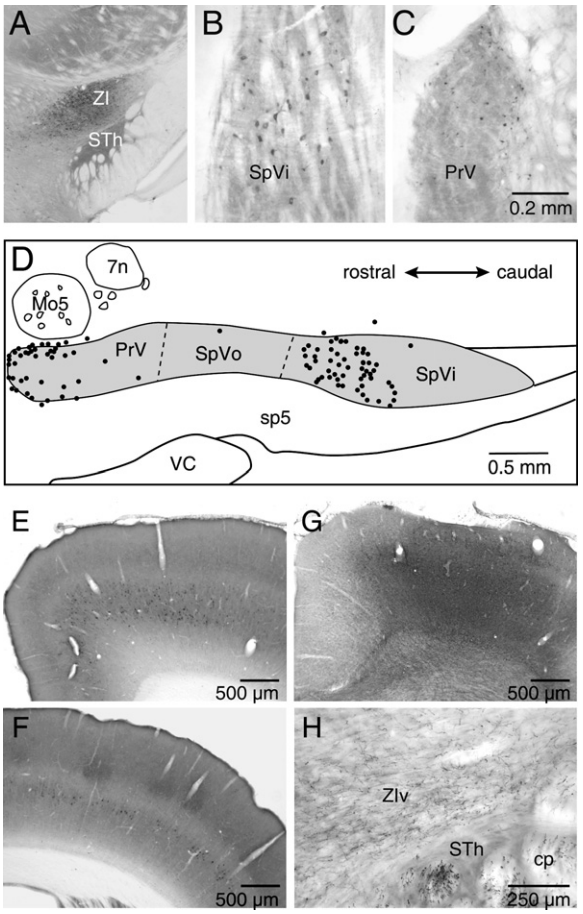

Figure 4. Origin of Trigeminal and Cortical Inputs to the ZIv

Following FluoroGold injection in ZI (coronal section in [A]), retrogradely labeled cells in the brainstem were found in the rostral part of the SpVi (horizontal section in [B]), and in the anterior pole of the PrV (horizontal section in [C]). The drawing in (D) shows the distribution of labeled neurons from two alternate horizontal sections of the brainstem. In the cortex, retrograde labeling was present in layer 5b of the motor (E) and somatosensory (F) areas. Pressure injection of BDA in the vibrissa motor area (G) labeled a dense plexus of fibers in ZIv (H). Photomicrographs in (E)–(H) were taken from coronal sections. 7n, facial nerve tract; cp, cerebral peduncle; Mo5, motor trigeminal nucleus; SpVo, oralis subnucleus of the spinal trigeminal complex; sp5, spinal trigeminal tract; STh, subthalamic nucleus; VC, ventral cochlear nucleus.

nucleus that also contains Po-projecting cells (Veinante et al., 2000a; Figures 4B and 4D). The caudal half of the SpVi, which projects to the VPMvl, did not contain any labeled cells. In rostral brainstem, retrograde labeling was present in the Kölliker-Fuse nucleus, and in the most anterior part of the PrV, particularly in the medial aspect of the nucleus where the nose and perioral regions are represented (Figures 4C and 4D); the ventral, whisker-like patterned region of the nucleus was notably devoid of retrogradely labeled cells (seven to ten cells per rat). These anatomical observations fully accord with results obtained in lesioned rats, confirming that the SpVi is the primary source of vibrissal input to the ZIv.

Motor Cortical Areas Are the Primary Source of Cortico-Incertal Projection to ZI

Next we addressed the question of how cortico-incertal inputs affect vibrissal responses in ZIv. As a first step, we mapped the distribution of cortical cells that give rise to cortico-incertal projections. Previous tract-tracing studies have shown that these projections arise principally from the cingulate cortex, which projects to the dorsal area of ZI (ZId), and from the motor and somatosensory areas, which project to both ZId and ZIv (Roger and Cadusseau, 1985; Mitrofanis and Mikuletic, 1999). However, none of these studies had provided a quantitative estimate of the respective contribution of the latter regions to ZIv innervation. We thus injected FluoroGold into the ZI of five rats to estimate the prevalence of retrogradely labeled cells in the motor and somatosensory areas. Three cases were analyzed, in which the injection sites were restricted to ZI with no or minimal diffusion to the subthalamic nucleus (same injection site as in Figure 4A). In those cases, all retrogradely labeled cells were located in layer 5b and, except for the cingulate cortex, the motor areas (regions labeled Fr1 and Fr2 in the atlas of Paxinos and Watson [1998]) contained the highest density of retrogradely labeled cells (Figure 4E). In the somatosensory areas (S1 and S2), retrograde labeling was discontinuous, since cells were most often, but not exclusively, clustered within the septal columns of S1 (Figure 4F). The numerical importance of the motor cortical projection is illustrated by the fact that a 500 μm wide column of tissue in a single section of the motor cortex (60 μm thick) contains as many retrogradely labeled cells (56 ± 5 cells, 5 alternate sections) as the full expanse of the somatosensory areas in single sections cut through the parietal cortex (60 ± 7 cells, 5 alternate sections). The importance of the motor cortex projection to ZI was further confirmed by the high density of terminal labeling found in ZI (particularly in ZIv) following biotinylated dextran amine (BDA) injections in the vibrissa motor area (n = 2 rats; Figures 4G and 4H). The density of terminals was highest in rostral and medial ZIv, and diminished gradually across the caudal and lateral sectors of the nucleus. Because different cortical areas innervate different sectors of ZI (Mitrofanis, 2005), we also examined to what extent the terminal territory of motor cortex afferents coincides with the spatial distribution of Po-projecting ZIv cells, and coincides with the location of incertal neurons that responded to vibrissa deflection. Figure 5 shows that retrogradely labeled cells from Po and the vast majority of vibrissa-sensitive ZIv cells labeled with Neurobiotin (n = 25) share a common territory, right above the lateral segment of the subthalamic nucleus (Figures 5B and 5D–5F). That territory contains a lower density of motor cortex terminals than the rostromedial aspect of ZIv does. On the basis of these anatomical results, we examined how stimulation of the vibrissa motor cortex affects sensory responses in ZIv.

Validation of the Experimental Approach

The wiring diagram of Figure S2 illustrates the corticofugal pathways through which motor cortex stimulation can

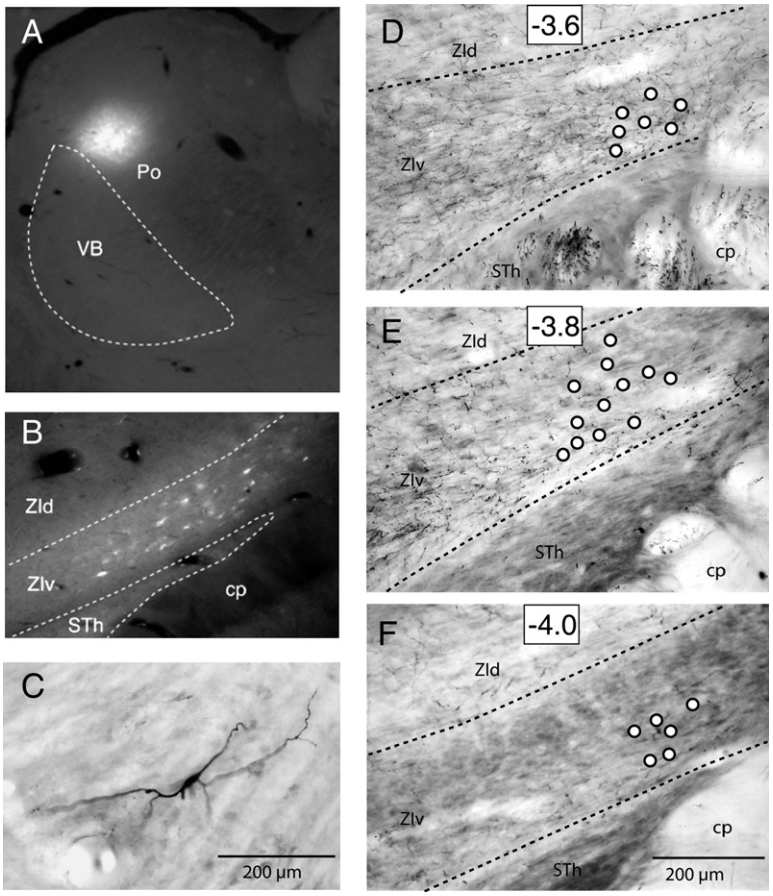

Figure 5. Comparative Localization of Zlv Cells that Project to Po and Those that Responded to Whisker Deflection

Injection of FluoroGold in Po (A) led to the retrograde labeling of Zlv cells right above the lateral segment of the subthalamic nucleus (B). (C) Photomicrograph of a Zlv cell juxtacellularly labeled with Neurobiotin. (D–F) Localization of 25 juxtacellularly stained whisker-responsive cells in the Zlv. Cell location (white dots) is superimposed upon CO-stained coronal sections in which terminals from the motor cortex had been labeled with BDA. Corresponding frontal planes refer to the distance behind the bregma. Note that whisker-responsive cells are also clustered right above the lateral segment of the subthalamic nucleus. STh, subthalamic nucleus; cp, cerebral peduncle; VB, ventrobasal complex.

affect sensory responses in Zlv. In addition to direct projections to Zl, the vibrissa motor cortex projects to several cortical regions, which include S1 and S2 that in turn project to the Zl and the SpVi (Welker et al., 1988; Jacquin et al., 1990; Miyashita et al., 1994; Izraeli and Porter, 1995; Veinante et al., 2000b). The recruitment of these parallel descending pathways by electrical stimulation of the motor area represents a confounding factor in assessing the direct action exerted by motor cortex on sensory transmission in Zlv. This was confirmed in pilot experiments that revealed complex and variable excitatory and inhibitory responses in Zlv for up to 50 ms after the onset of the cortical stimulus (data not shown). Recordings in the SpVi also revealed that a majority of cells were excited by cortical stimulation at latencies of 12–20 ms (Figure S2B). When whisker deflection was delivered after the excitation, vibrissal responses were strongly depressed. Because motor cortex has no direct connections with the sensory trigeminal nuclei (Miyashita et al., 1994), these responses were likely mediated by the activation of corticofugal cells of the somatosensory cortical areas, which project to the SpVi (Welker et al., 1988; Jacquin et al., 1990). An extensive lesion of the parietal areas that included S1, S2, and the underlying subcortical white matter produced a complete suppression of the excitatory and inhibitory responses (Figure S2C; the spatial extent of the lesion is shown in Figure S3). Changing the site of stimulation in the motor area (six different sites) or increasing stimulus intensity up to four times the threshold for provoking whisker motion (protraction or retraction) did not modulate any of the 56 interpolaris cells tested in two lesioned rats. We thus used this lesioned preparation to examine the effect of motor cortex stimulation on the vibrissal responses of Zlv neurons.

Motor Cortex Stimulation Suppresses Vibrissal Responses in Zlv

The rate of spontaneous discharges of Zlv cells in S1/S2 lesioned rats was much lower (<1 Hz) than that observed in normal rats under the same anesthetic condition (~10 Hz). Yet, cells maintained brisk and consistent responses to ramp-and-hold whisker deflection. Single-shock stimulation of the motor cortex induced excitatory responses whose magnitude and consistency varied with the location of the incertal units. The strongest responses were observed in vibrissa-insensitive cells located just rostral and medial to those activated by the whiskers (i.e., in the motor subsector of Zlv). In 55% of these cells (n = 33), response consisted of a barrage of four to seven action potentials (mean latency of the first spike: 5.2 ± 0.2 ms; barrage duration: up to 25 ms; Figure 6A). In vibrissa-sensitive units, however, excitatory responses were either

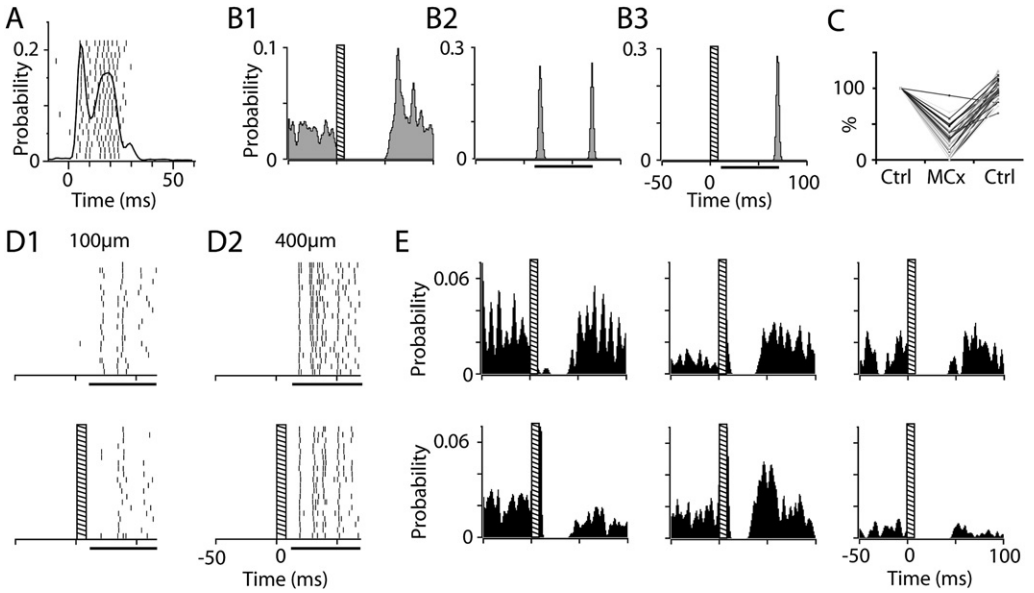

Figure 6. Motor Cortex Suppresses Vibrissal Responses in ZIv

(A) Motor cortex stimulation (single shock) induced a barrage of action potentials in most cells recorded in the motor subsector of the ZIv (raster in A). A population PSTH (n = 33 cells) is superimposed over the raster in (A). In contrast, motor cortex stimulation (three shocks; hatched bar) suppressed spike discharges induced by juxtacellular injection in a representative vibrissa-sensitive cell (B1). Whisker deflection (horizontal black bar in [B2]) induced on/off responses in the same ZIv cell. The on response was totally suppressed by prior stimulation of the motor cortex (hatched bar; [B3]). The graph in (C) shows how normalized response magnitude, as estimated by the mean number of spikes per deflection, was reduced by motor cortex stimulation (MCx) in a population of 37 ZIv cells (mean suppression: 71.5% ± 3.4%). Vibrissal responses induced by small-amplitude whisker deflection (D1) were more strongly suppressed by motor cortex stimulation than those elicited by large-amplitude deflection of the same vibrissa (D2). (E) Background activity induced in six different ZIv cells by a continuous air jet (left and middle columns) or pink noise vibration (right column) was completely suppressed by motor cortex stimulation.

absent or consisted most often of a single action potential. When the latter cells were induced to fire by juxtacellular current injection, trains of cortical stimuli produced a marked suppression of background discharges that lasted for up to 40 ms after stimulus onset (Figure 6B1; see also group PSTH in Figure 8C; percent suppression between 15–25 ms after stimulus onset: 92.8% ± 4.5%; between 15–35 ms: 67.1% ± 9.1%; n = 26 cells). Likewise, when whisker deflection was delivered 15 ms after the onset of the cortical stimulus, vibrissal responses were markedly depressed. In the example shown in Figures 6B2 and 6B3, the mean number of spikes per deflection in a 20 ms time window after the onset of deflection passed from 2.5 to 0, and recovered to 2.4 after the pairing test. The graph of Figure 6C shows how normalized response magnitude, as estimated by the mean number of spikes per deflection, was reduced by motor cortex stimulation in a population of 37 ZIv cells (mean suppression: 71.5% ± 3.4%).

Although motor cortex-induced suppression of vibrissal responses was observed in all of the incertal units tested, the magnitude of suppression in individual cells proved to be highly dependent on stimulus parameters: the intensity and site of motor cortex stimulation; the whisker that was stimulated within the receptive field; and the direction, amplitude, and velocity of deflection. In general, complete suppression was only obtained with low-amplitude whisker deflection. A representative case is shown in Figures 6D1 and 6D2, where response to 0.1 mm deflection of whisker B2 was suppressed by 82%, while that evoked by 0.4 mm deflection of the same vibrissa was suppressed by only 17%.

High-velocity whisker deflection, similar to that used in the present study, evokes a short-latency burst of action potentials in interpolaris cells (intraburst frequency: 300–900 Hz; Furuta et al., 2006), and interpolaris axons establish large synaptic contacts with multiple release sites on the soma and proximal dendrites of ZIv cells (Lavallée et al., 2005). It thus seems unlikely that incertal inhibition evoked by motor cortex could ever succeed in completely suppressing the strong vibrissal responses produced by high-velocity deflection of a whisker. Therefore, we also examined whether sensory responses induced by low-amplitude vibration of a whisker could be totally suppressed by motor cortex stimulation. This test was carried out in 10 ZIv cells that were induced to fire by applying pink noise vibration (20–200 Hz) to a single whisker, or by wiggling the tip of several whiskers with a continuous pulsed air jet. Parameters of sensory stimuli were adjusted to induce sustained discharges in the range of 8–20 Hz. In all cells tested in this manner, motor cortex stimulation produced a complete arrest of the

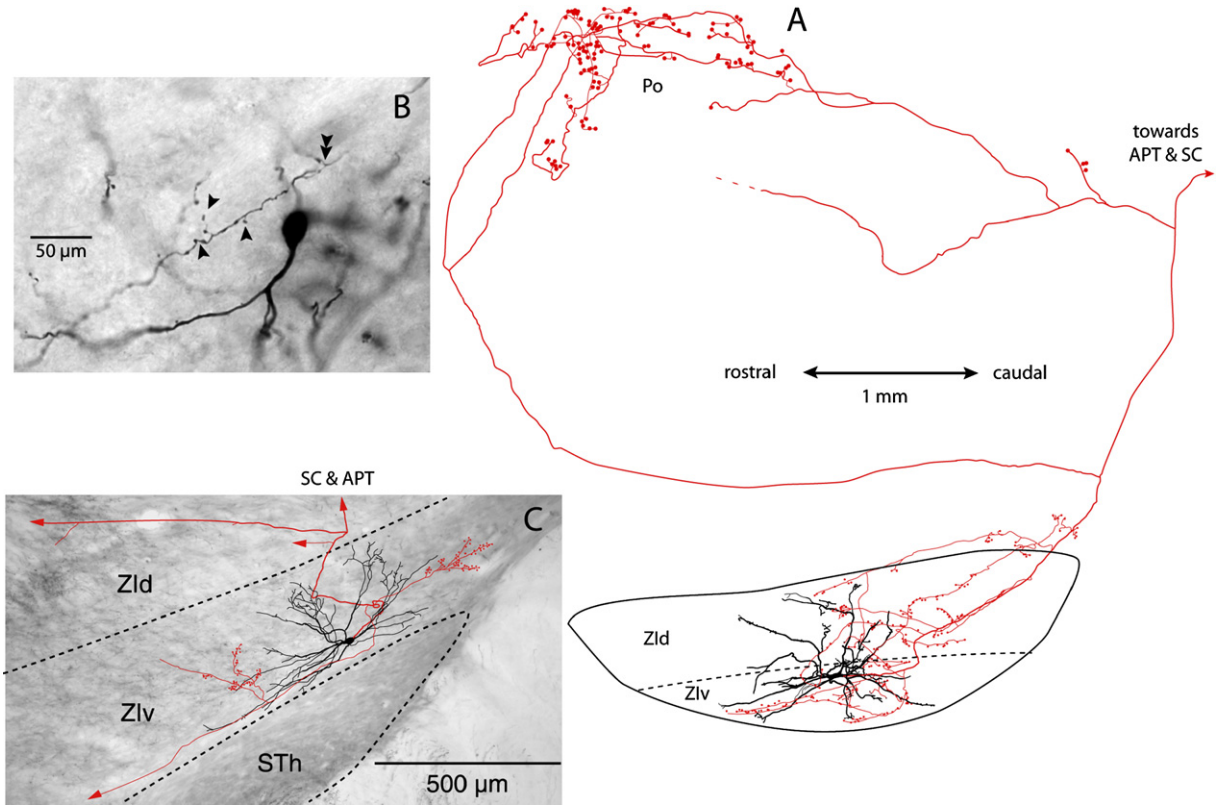

Figure 7. Local Axon Collaterals Given Off by Incertal Cells

(A) Drawing of a ZIv cell that was labeled with BDA. The reconstruction was made from serial parasagittal sections, so that the dendritic tree, in black, appears to spread in ZId because of the curved structure of the nucleus. The axon, in red, gives off a rich network of collaterals with boutons within the ZI, and also projects to the Po, the APT, and the superior colliculus. Photomicrograph in (B) shows local axon collaterals given off by another ZIv cell. Double arrowhead indicates an axonal branch point, and single arrowheads point to local boutons. (C) Reconstruction of another vibrissa-sensitive ZIv cell that project to the APT and superior colliculus. The drawing was overlain on a corresponding section stained for CO. Note again the presence of axonal branches and terminals in the ZIv (in red). Photomicrographs (B) and (C) were taken from a coronal section. SC, superior colliculus.

discharges that lasted for 20–40 ms after stimulus onset (Figure 6E).

Response Suppression in ZIv Is Mediated by an Intra-Incertal GABAergic Network

We next addressed the origin of motor cortex-induced inhibition in ZIv. On the basis of anatomical studies, two brain regions receive input from the vibrissa motor cortex and contain GABAergic cells that could potentially inhibit ZIv neurons. These are the anterior pretectal nucleus (APT) and the ZI itself (Miyashita et al., 1994; Bokor et al., 2005). After complete lesion of the ipsilateral APT (Figure S4), motor cortex stimulation still suppressed current-induced discharges and vibrissal responses in 21 out of 24 cells tested in two rats, which suggested that inhibition might be mediated by an intra-incertal circuit.

One anatomical study (Power and Mitrofanis, 1999) already documented the presence of a dense meshwork of axon collaterals in the ZI. It remained unclear, however, whether these axonal branches were actually issuing from ZI axons, and whether they arose from ZId or ZIv neurons. To settle this issue we reconstructed the axons of 17 ZIv and 28 ZId neurons that had been individually labeled either with Neurobiotin in our current experiments, or with BDA in a previous study (S. Richard et al., 2002, Soc. Neurosci., abstract). The dendroarchitecture of these cells conformed to the detailed description recently published by Barthó et al. (2007). Reconstructions made from CO-stained sections revealed that any single ZI cell projects to at least two of the following structures: the thalamus, the APT, the superior colliculus, or other brain regions. All labeled cells also supplied axonal branches with strings and clusters of boutons within the ZI itself (Figures 7A–7C). Local collaterals issuing from most ZId axons were restricted to the dorsal division of the nucleus; few cells innervated the ZIv, in which they gave off scattered boutons. In contrast, all ZIv cells distributed boutons (1–3 µm in diameter) within both the ventral and dorsal divisions of ZI. Figure 7A shows the reconstruction of a particularly well-stained ZIv neuron that projected locally in ZI, as well as to the Po, the APT, and the superior

colliculus. Among the whole population of cells reconstructed, none displayed features of local circuit cells with axonal projections restricted to the ZI.

Since the vast majority of ZIv cells are GABAergic, intra-ZIv collaterals provide a substrate for a mechanism of lateral inhibition. Therefore, one would expect motor cortex-induced inhibition in ZIv to be depressed by gabazine, a specific antagonist at GABAa receptors. After local injection of gabazine in ZIv (100 nl of a 5 mM solution in saline; n = 2 rats), incertal cells displayed a pronounced increase in spontaneous firing rate (mean rate: 52.6 ± 10.7 Hz; n = 8 cells) that slowly recovered to control value (~1 Hz) after 2 hr. During that period cortical stimulation became totally ineffective in suppressing background discharges (n = 13 vibrissa-sensitive cells). Instead, inhibition was replaced by a massive, long-lasting excitation (Figure 8A). Group PSTHs of Figures 8B and 8C show the dramatic reversal of the inhibitory effect produced by gabazine. The PSTH in Figure 8D is a rescaled version of the PSTH shown in Figure 6A. It shows the close time relationship between inhibition induced by motor cortex in vibrissa-sensitive cells (Figure 8C), and the excitatory responses of vibrissa-insensitive cells in the motor subsector of ZIv. Behaviorally, gabazine injection triggered episodic contractions of the eyelids, facial muscles, and lower jaw, which rendered unfeasible the application of controlled vibrissa deflection.

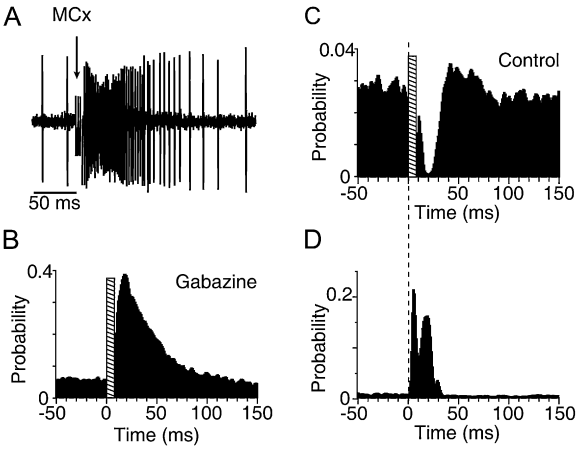

Figure 8. Blockade of Intra-Incertal Inhibition by Gabazine
After pressure injection of gabazine in the ZIv, whisker-sensitive cells responded to motor cortex stimulation with a prominent excitation ([A]; population PSTH of 13 cells in [B]). Population PSTH in (C) shows the inhibition induced in 26 ZIv cells by motor cortex stimulation in normal rats. Background discharges in these cells were driven by juxtacellular current injection. The PSTH in (D) is a rescaled version of the PSTH shown in Figure 6A. It shows the close time relationship between inhibition induced by motor cortex in vibrissa-sensitive cells (C) and the excitatory responses recorded in vibrissa-insensitive cells in the motor subsector of ZIv.

DISCUSSION

ZI is among the least studied regions of the brain; its name does not even appear in the index of many textbooks. It is involved in a variety of behaviors such as visceral activity (ingestive and sexual), arousal, posture and locomotion, and eye movements (see review by Mitrofanis, 2005), which probably explains why we are uncertain about what it actually does. ZI contains cytoarchitectonic divisions with an exceptionally diverse chemoarchitecture, but the ventral division remains the most distinguishable due to its CO reactivity and high content of parvalbumine-positive GABAergic cells (Kolmac and Mitrofanis, 1999; Lavallée et al., 2005). Superimposed upon cytoarchitectonic divisions, there is a set of modality subsectors (visual, auditory, somatosensory) and a prominent motor subsector (Nicolelis et al., 1992; Mitrofanis and Mikuletic, 1999; Shaw and Mitrofanis, 2002). All incertal cells labeled in the present study displayed widespread dendritic arbors (dendritic field span ~800 μm; see also Barthó et al., 2007), and each axon gave off collaterals that arborized locally within the ZI, which provides an anatomical structure for a mechanism of lateral inhibition. Thus, ZIv appears as a network of GABAergic cells with widespread interconnections, so that cells in one subsector may influence the activity of cells in a different subsector. This is clearly demonstrated by our results, which show that cells in the motor subsector were excited by motor cortex stimulation, whereas those in the "vibrissal subsector" were inhibited. Inhibition was blocked by gabazine, and persisted after lesion of the other putative inhibitory inputs. Therefore, together with the aforementioned anatomical data, these results clearly indicate that vibrissal responses in ZIv are suppressed by a mechanism of lateral inhibition.

Disinhibition and Whisker Motion

The degree of vibrissal response suppression after motor cortex stimulation strongly depended on the parameters of vibrissa deflection. Complete suppression mostly occurred for responses elicited by low-amplitude (velocity) stimuli. However, total suppression is theoretically required for disinhibition to occur in Po. This raises the question of whether high-velocity deflection that mimics the impact of whisker contact during a whisk is a realistic stimulation protocol for assessing the validity of the top-down disinhibitory hypothesis. Although rats whisk to navigate and locate objects, they commonly adopt a different strategy to gather fine-grained tactual information (Krupa et al., 2001). Videographic analysis of whisker motion in behaving rats revealed that during object palpation rats use a strategy of minimum impact (Carvell and Simons, 1995; Mitchinson et al., 2007), just as humans do when exploring surface texture with their fingertips. Therefore, disinhibition in Po should be time related to vibrissal inputs that are contingent on motor instructions that control fine whisker motion during palpation (i.e., the object recognition mode discussed by Curtis and Kleinfeld [2006]). Conversely, afferent inputs that signal whisker contact during large-amplitude whisks (i.e., the exploratory mode) should still be gated by the incerto-thalamic pathway.

Top-Down versus State-Dependent Gating Mechanism

Several ascending pathways of information processing have been so far identified in the vibrissal system of rodents (see Yu et al., 2006). Each of these pathways arises from a specific population of brainstem trigeminal neurons, transits through a different thalamic region, and has its own areal and laminar distribution in the neocortex. Although there is general consensus that the lemniscal pathway serves texture and shape discrimination, the respective functional role of the other pathways remains an open issue. This is the case of the paralemniscal pathway that transits through Po, in which the relay of sensory messages is gated by inhibitory inputs from the ZIv (Trageser and Keller, 2004; Lavallée et al., 2005). Because the vibrissa-recipient zone of Po receives input from, and projects to, the motor cortex, it was proposed that the paralemniscal pathway conveys sensory information that is contingent on motor instructions that control whisker motion (Lavallée et al., 2005). This possibility receives further support from the present study, in which we show that corticofugal messages from the vibrissa motor cortex can suppress vibrissal responses in ZIv, thus relieving Po from incertal inhibition, and allowing the relay of sensory information to cortex. Yet, conclusive evidence for this hypothesis is currently lacking. Our attempts to record the disinhibitory effect of motor cortex stimulation in Po were fruitless. The major difficulty is that electrical stimulation of the vibrissa motor cortex not only activates layer 5 cells that project to ZI, but also lamina 6 cells that project to Po and to the associated sector of the reticular thalamic nucleus (Deschênes et al., 1998). Inhibition of reticular thalamic origin kept suppressing vibrissal responses in Po when we paired vibrissa deflection with motor cortex stimulation. Therefore, for the moment, our results should be considered as a proof of the concept that sensory transmission in Po involves a top-down disinhibitory mechanism.

Sensory transmission through Po was also proposed to be state dependent, relying on inhibition of incertal cells produced by brainstem cholinergic neurons that increase their firing rate on arousal (Trageser et al., 2006). A state of arousal, however, does not merely rely on a cholinergic modulation of central circuits. Incertal cells also receive profuse excitatory inputs from layer 5 corticofugal neurons that also increase their firing rate on arousal (Steriade and McCarley, 1990). Because this corticofugal drive can balance out cholinergic inhibition, it remains unclear whether ZIv cells will indeed fail to respond to sensory stimuli in an awake animal. Recordings in head-restrained, nonanesthetized cats did not reveal any change in spontaneous firing rates of incertal cells across the sleep/waking cycle, but changes in firing rates were reported to occur in conjunction with limb movements (Steriade et al., 1982). Yet, the top-down disinhibitory mechanism will obviously operate during the waking state; therefore, the two hypotheses are not mutually exclusive. Actually, acetylcholine release could further aid in reducing cells' excitability in ZI, thus contributing to lessening the impact of incertal inhibition in Po.

Functional Significance

A central issue in sensory physiology is to understand how an animal endowed with highly sensitive sensory organs with which it explores the environment can control the unceasing stream of sensory inputs it receives, and select those that are most relevant to an adaptive behavior. Clearly, there should exist multilevel, state-dependent, and context-dependent gating mechanisms that filter out irrelevant sensory inputs. Our results suggest that corticofugal pathways that control incerto-thalamic circuits might be directly involved in selecting sensory inputs that are conveyed to the cerebral cortex by the paralemniscal pathway. Yet, to achieve conclusive evidence for this top-down control, there is a crucial need for physiological information about how cells behave in freely ranging animals that engage in biologically relevant tactile behaviors.

EXPERIMENTAL PROCEDURES

Experiments were conducted in accordance with federally prescribed animal care and use guidelines. The University Committee for Animal Use in Research approved all experimental protocols. Experiments were carried out in 65 male and 3 female rats (250–300 g; Sprague Dawley) under ketamine (75 mg/kg)/ xylazine (5 mg/kg) anesthesia. The left facial nerve was cut, and the rat was placed in a stereotaxic apparatus. The animal breathed freely, and body temperature was maintained at 37.5°C with a heating pad controlled thermostatically. Throughout the experiment, a deep level of anesthesia was maintained (stage III-3, Friedberg et al., 1999) by additional doses of anesthetics given at 1 hr intervals (ketamine 20 mg/kg plus xylazine 0.3 mg/kg, i.m.).

Single units were recorded extracellularly with micropipettes (0.5–1 μm) filled with a solution of potassium acetate (0.5 M) and Neurobiotin (2%, Vector Laboratories, Burlingame, CA). Signals were amplified, band-pass filtered (200 Hz to 3 kHz), and sampled at 10 kHz. In most experiments cell location was assessed by the juxtacellular labeling of at least one unit (Pinault, 1996). At the end of the experiments, rats were perfused under deep anesthesia with saline, followed by a fixative containing 4% paraformaldehyde in phosphate buffer (PB 0.1 M, pH 7.4). Brains were postfixed for 2 hr, cryoprotected in 30% sucrose, and cut at 60 or 70 μm on a freezing microtome. Sections were processed for CO and Neurobiotin histochemistry according to standard protocols that were described in detail previously (Veinante et al., 2000a).

Cortical Inactivation

In five rats, we investigated the effect of silencing the barrel cortex on vibrissal responses in ZIv. The EEG activity of the barrel cortex was monitored with a pair of tungsten microelectrodes, and cortical silencing was produced by topical application of a drop of KCl (1 M) over the pia. Recovery of normal activity occurred spontaneously, or was aided by local rinse with saline.

Electrolytic and Silver Nitrate Lesions

Electrolytic lesions of brainstem nuclei and of the APT were carried out by passing DC (2 mA, 2 s) through a tungsten electrode (shaft diameter, 200 μm; tip diameter, 50 μm; deinsulated over 1 mm). We used the stereotaxic coordinates of the atlas of Paxinos and Watson (1998), and current was passed at multiple depths along 2–4 descents 400 μm apart to fully destroy the targeted regions.

S1 and S2 somatosensory areas were lesioned by the application of a small crystal of silver nitrate over the pia (Lavallée et al., 2005). The crystal was left in place for 20 min to allow diffusion of the chemical to the subcortical white matter. Then, the cortical surface was abundantly rinsed with saline. Silver nitrate is a strong cauterizing agent that burns tissue; this type of lesion does not produce any bleeding or tissue swelling. After aldehyde fixation, the burnt tissue becomes brownish but turns black after CO processing. The extent of the lesion clearly showed up in the histological material as a deep black region.

Vibrissa and Motor Cortex Stimulation

Vibrissae were cut at 10 mm from the skin, and we assessed the receptive field size of single units by deflecting individual vibrissae with a hand-held probe under a dissecting microscope. An audio monitor and a computer display were used to monitor the responses. The tip of a vibrissa was then inserted into the groove of a beveled straw attached to a ceramic bimorph bender (Physik Instrumente, Karlsruhe, Germany). The vibrissa was pushed in a given direction at stimulus onset, but returned passively to a neutral position at stimulus offset. Ramp-and-hold waveforms (rise/fall times, 5 ms; total duration, 50 ms; amplitude, 50–500 μm; angular velocity, up to 1000°/s; interstimulus interval, 1 s) were used to deflect vibrissae from their resting position in four directions spanning 360° (i.e.., in 90° increments relative to the horizontal alignment of the vibrissa rows). As measured with a photodiode, resonance frequency was 180 Hz (amplitude, 5% of peak displacement; i.e., 20 μm for the first period). Stimuli were repeated 20 times, the probe was rotated by 90°, and the sequence was repeated. This procedure was applied to each of the vibrissae that compose the receptive field of a cell. In about 20% of the cases, the threshold for eliciting responses required deflection amplitude (velocity) that exceeded the performance of the stimulator.

In some experiments vibrissae were stimulated in a sustained manner by applying pink noise vibration (20–200 Hz) to the cut tip of a vibrissa, or by directing a gentle air jet toward the distal end of the uncut vibrissae. For noise vibration, the tip of a vibrissa was inserted into a cone-shaped glass bead attached to the piezo bender (Deschênes et al., 2003). The noise profile and its frequency content are shown in Figure S5. A small compressor (aquarium pump) was used to deliver a weak airflow toward the distal tip of the vibrissae. Motion of whisker C2 produced by the airflow was measured ex vivo with a CCD array. The array captured motion at about 1.5 cm from the tip of the vibrissa. Figure S5 shows a bout of vibrissa motion together with its fast Fourier transform.

The motor cortex was stimulated with a pair of glass-insulated platinum/iridium microelectrodes (FHC, Bowdoin, ME). Stimuli consisted of three shocks (pulse duration, 200 μs; frequency, 330 Hz) at current intensity that elicited whisker motion (retraction or protraction; intensity, 75–350 μA).

Data Analysis

Spike events elicited by vibrissal stimulation were collected in PSTHs of 20 responses with 0.2 ms bin width. The number of spikes evoked within a time window of 10 ms after stimulus onset was used to assess response magnitude. The latency of response onset was estimated as the bin corresponding to 0.5 of peak value of the PSTH (bin width, 0.2 ms) after three-bin smoothing with a boxcar kernel.

Two methods were used to assess the inhibitory effect of motor cortex stimulation on ZIv neurons. Once a unit was isolated, the micropipette was advanced until spike amplitude reached 5–8 mV. From that juxtacellular position, positive DC (1–4 nA) was applied to induce tonic discharges (10–25 Hz). Spike suppression was assessed during this background activity by stimulating motor cortex at 1 s intervals. Spike events were collected into PSTHs of 100–125 responses with 1 ms bin widths. The presence of inhibitory responses was assessed by comparing firing rates within time windows of 10 and 20 ms after stimulus onset to prestimulus firing rates estimated over a 100 ms period. To accommodate the latency of inhibition, the start of these windows was offset by 15 ms from the start of the stimulus. The magnitude of inhibition was rated as the percent difference in the mean number of counts per bin during the prestimulus and poststimulus time windows.

A conditioning-test procedure was employed to assess the inhibition of vibrissal responses by motor cortex. A control PSTH of 20 vibrissal responses was computed, and a second PSTH was built by delivering whisker deflection 15 ms after the onset of the cortical stimulus. Inhibition was rated as the percent suppression in the mean number of spikes per deflection. Artifacts of motor cortex stimuli did not allow us to discriminate the short-latency action potentials occurring during the train of stimulation; although these spikes were clearly discernible on the oscilloscope screen, they were removed, together with the artifacts from the PSTHs.

Data were analyzed with Neuroexplorer (Plexon, Dallas, TX), and Excel (Microsoft, Redmond, WA) software. The angular tuning of vibrissal responses was assessed using circular statistics (Oriana 2.0; KCS, Anglesey, GB). Unless otherwise stated, results are reported as mean ± SEM.

Tract Tracing Experiments

FluoroGold (Fluorochrome Inc., Denver, CO) was injected iontophoretically in the Po (n = 3 rats) or the ZI (n = 5 rats). The tracer was delivered by passing depolarizing current pulses (1 μA, 2 s duty cycle for 20 min) through micropipettes (diameter, 25 μm) filled with 2% FluoroGold dissolved in cacodylate buffer (0.1 M, pH 7). After a survival period of 2 days, rats were perfused as above; sections were stained for CO, and processed for FluoroGold immunohistochemistry. After preincubation for 1 hr in PBS with 3% normal goat serum and 0.3% Triton X-100, sections were incubated overnight in the same mixture containing an anti-FluoroGold antiserum (1:8000; Chemicon, Temecula, CA). The antibody was revealed using a peroxidase-labeled secondary antibody (goat IgG; Chemicon) and nickel-3, 3 -diaminobenzidine tetrahydrochloride (Ni-DAB) as a substrate.

Two rats were used to map the cortico-incertal projections of the motor cortex. The vibrissa motor cortex was identified by microstimulation, and 2 μl BDA (2% BDA-10,000 in PBS; Molecular Probes, Eugene, OR) was pressure injected into layer 5 (depth, 1400 μm). After a survival period of 5 days, rats were deeply anesthetized and perfused as above. Coronal sections through the thalamus were stained for CO, and incubated with the avidin-biotinylated-horseradish peroxidase complex (ABC; Vector Laboratories, Burlingame, CA) in Tris-buffered saline for 4 hr, and developed in Ni-DAB.

Additional material was provided by colleagues who gave us access to a collection of incertal cells that had been juxtacellularly labeled with BDA (S. Richard et al., 2002, Soc. Neurosci., abstract). Cells labeled with biotylinated tracers were reconstructed from serial sections with a camera lucida. Photomicrographs were taken with a Spot RT camera (Diagnostic Instruments Inc., Sterling Heights, MI), and imported in Photoshop 7.0 (Adobe Systems Inc., San Jose, CA) for contrast and brightness adjustments.

Supplemental Data

The Supplemental Data for this article can be found online at http://www.neuron.org/cgi/content/full/56/4/714/DC1/.

ACKNOWLEDGMENTS

This work was supported by a grant (MT-5877) from the Canadian Institute of Health Research to M.D. We are grateful to Mme. Sandra Richard and Dr. André Parent, who gave us access to their histological material.

Received: July 16, 2007
Revised: September 12, 2007
Accepted: October 17, 2007
Published: November 20, 2007

REFERENCES

Barthó, P., Freund, T.F., and Acsády, L. (2002). Selective GABAergic innervation of thalamic nuclei from zona incerta. Eur. J. Neurosci. *16*, 999–1014.

Barthó, P., Slézia, A., Varga, V., Bokor, H., Pinault, D., Buzsáki, G., and Acsády, L. (2007). Cortical control of zona incerta. J. Neurosci. *27*, 1670–1681.

Bokor, H., Frère, S.G., Eyre, M.D., Slézia, A., Ulbert, I., Lüthi, A., and Acsády, L. (2005). Selective GABAergic control of higher-order thalamic relays. Neuron *45*, 929–940.

Carvell, G.E., and Simons, D.J. (1995). Task- and subject-related differences in sensorimotor behavior during active touch. Somatosens. Mot. Res. *12*, 1–9.

Curtis, J.C., and Kleinfeld, D. (2006). Seeing what the mouse sees with its vibrissae: a matter of behavioral state. Neuron *50*, 524–526.

Deschênes, M., Veinante, P., and Zhang, Z.-W. (1998). The organization of corticothalamic projections: reciprocity versus parity. Brain Res. Brain Res. Rev. *28*, 286–308.

Deschênes, M., Timofeeva, E., and Lavallée, P. (2003). The relay of high-frequency sensory signals in the whisker-to-barreloid pathway. J. Neurosci. *23*, 6778–6787.

Friedberg, M.H., Lee, S.M., and Ebner, F.F. (1999). Modulation of receptive field properties of thalamic somatosensory neurons by the depth of anesthesia. J. Neurophysiol. *81*, 2243–2252.

Furuta, T., Nakamura, K., and Deschênes, M. (2006). Angular tuning bias of vibrissa-responsive cells in the paralemniscal pathway. J. Neurosci. *26*, 10548–10557.

Guillery, R.W. (2005). Anatomical pathways that link perception and action. Prog. Brain Res. *149*, 235–256.

Izraeli, R., and Porter, L.L. (1995). Vibrissal motor cortex in the rat: connections with the barrel field. Exp. Brain Res. *104*, 41–54.

Jacquin, M.F., Wiegand, M.R., and Renehan, W.E. (1990). Structure-function relationships in rat brain stem subnucleus interpolaris. VIII. Cortical inputs. J. Neurophysiol. *64*, 3–27.

Kolmac, C.I., and Mitrofanis, J. (1999). Distribution of various neurochemicals within the zona incerta: an immunocytochemical and histochemical study. Anat. Embryol. (Berl.) *199*, 265–280.

Kolmac, C.I., Power, B.D., and Mitrofanis, J. (1998). Patterns of connections between zona incerta and brainstem in rats. J. Comp. Neurol. *396*, 544–555.

Krupa, D.J., Matell, M.S., Brisben, A.J., Oliveira, L.M., and Nicolelis, M.A.L. (2001). Behavioral properties of the trigeminal somatosensory system in rats performing whisker-dependent tactile discriminations. J. Neurosci. *21*, 5752–5763.

Lavallée, P., Urbain, N., Dufresne, C., Bokor, H., Acsády, L., and Deschênes, M. (2005). Feedforward inhibitory control of sensory information in higher-order thalamic nuclei. J. Neurosci. *25*, 7489–7498.

Masri, R., Trageser, J.C., Bezdudnaya, T., Li, Y., and Keller, A. (2006). Cholinergic regulation of the posterior medial thalamic nucleus. J. Neurophysiol. *96*, 2265–2273.

Mitchinson, B., Martin, C.J., Grant, R.A., and Prescott, T.J. (2007). Feedback control in active sensing: rat exploratory whisking is modulated by environmental contact. Proc. Biol. Sci. *274*, 1035–1041.

Mitrofanis, J. (2005). Some certainty for the "zone of uncertainty"? Exploring the function of the zona incerta. Neuroscience *130*, 1–15.

Mitrofanis, J., and Mikuletic, L. (1999). Organisation of the cortical projection to the zona incerta of the thalamus. J. Comp. Neurol. *412*, 173–185.

Miyashita, E., Keller, A., and Asanuma, H. (1994). Input-output organization of the rat vibrissal motor cortex. Exp. Brain Res. *99*, 223–232.

Nicolelis, M.A.L., Chapin, J.K., and Lin, R.C. (1992). Somatotopic maps within the zona incerta relay parallel GABAergic somatosensory pathways to the neocortex, superior colliculus, and brainstem. Brain Res. *577*, 134–141.

Nicolelis, M.A.L., Chapin, J.K., and Lin, R.C. (1995). Development of direct GABAergic projections from the zona incerta to the somatosensory cortex of the rat. Neuroscience *65*, 609–631.

Paxinos, G., and Watson, W. (1998). The Rat Brain in Stereotaxic Coordinates, Fourth Edition (London: Academic Press).

Pinault, D. (1996). A novel single-cell staining procedure performed in vivo under electrophysiological control: morpho-functional features of juxtacellularly labeled thalamic cells and other central neurons with biocytin or Neurobiotin. J. Neurosci. Methods *65*, 113–136.

Power, B.D., and Mitrofanis, J. (1999). Evidence for extensive interconnections within the zona incerta in rats. Neurosci. Lett. *267*, 9–12.

Power, B.D., Kolmac, C.I., and Mitrofanis, J. (1999). Evidence for a large projection from the zona incerta to the dorsal thalamus. J. Comp. Neurol. *404*, 554–565.

Roger, M., and Cadusseau, J. (1985). Afferents to the zona incerta in the rat: a combined retrograde and anterograde study. J. Comp. Neurol. *241*, 480–492.

Shaw, V.E., and Mitrofanis, J. (2002). Anatomical evidence for somatotopic maps in zona incerta of rat. Anat. Embryol. (Berl.) *206*, 119–130.

Steriade, M., and McCarley, R.W. (1990). Brainstem Control of Wakefulness and Sleep (New York: Plenum).

Steriade, M., Parent, A., Ropert, N., and Kitsikis, A. (1982). Zona incerta and lateral hypothalamic afferents to the midbrain reticular core of cat - HRP and electrophysiological study. Brain Res. *238*, 13–28.

Taylor, W.R., and Vaney, D.I. (2002). Diverse synaptic mechanisms generate direction selectivity in the rabbit retina. J. Neurosci. *22*, 7712–7720.

Trageser, J.C., and Keller, A. (2004). Reducing the uncertainty: gating of peripheral inputs by zona incerta. J. Neurosci. *24*, 8911–8915.

Trageser, J.C., Burke, K.A., Masri, R., Li, Y., Sellers, L., and Keller, A. (2006). State-dependent gating of sensory inputs by zona incerta. J. Neurophysiol. *96*, 1456–1463.

Veinante, P., and Deschênes, M. (1999). Single- and multi-whisker channels in the ascending projections from the principal trigeminal nucleus in the rat. J. Neurosci. *19*, 5085–5095.

Veinante, P., Jacquin, M.F., and Deschênes, M. (2000a). Thalamic projections from the whisker-sensitive regions of the spinal trigeminal complex in the rat. J. Comp. Neurol. *420*, 233–243.

Veinante, P., Lavallée, P., and Deschênes, M. (2000b). Corticothalamic projections from layer 5 of the vibrissal barrel cortex in the rat. J. Comp. Neurol. *424*, 197–204.

Welker, E., Hoogland, P.V., and Van der Loos, H. (1988). Organization of feedback and feedforward projections of the barrel cortex: a PHA-L study in the mouse. Exp. Brain Res. *173*, 411–435.

Williams, M.N., Zahm, D.S., and Jacquin, M.F. (1994). Differential foci and synaptic organization of the principal and spinal trigeminal projections to the thalamus in the rat. Eur. J. Neurosci. *6*, 429–453.

Yu, C., Derdikman, D., Haidarliu, S., and Ahissar, E. (2006). Parallel thalamic pathways for whisking and touch signals in the rat. PLoS Biol. *4*, e124. 10.1371/journal.pbio.0040124.